Annealing Effects on Thermal Diffusivity and Electrical Resistivity of a Surrogate for Metallic Fuel

Naoya ODAIRA* **and Yuji ARITA****

(Received September 20, 2019)

U-TRU-Zr metallic fuel is a candidate innovative fuel for the TRU burner. Americium (Am), one of the main targets of burning, will diffuse and form precipitates. The matrix and thermal properties of metallic fuels will change during high-temperature irradiation and annealing. In this study, the property changes of metallic fuels (including Am) were investigated by using surrogate elements. Niobium and rare earth (RE) elements were used as surrogates of U and Am. The thermal diffusivity and the electrical resistivity were measured for Nb-Zr+RE (5 wt.% of Ce or Nd) alloy specimens prepared by means of arc melting and then annealed at 400 °C.

Despite the similarity between the thermal diffusivity values, the electrical resistivity of the Nb-Zr+Ce alloy was significantly higher than that of the RE-free Nb-Zr alloy. Annealing had only a slight effect on the diffusivity, but yielded considerable improvement in the resistivity of the Ce-added specimens. The thermal diffusivity and electrical resistivity of the Nb-Zr+Nd alloy were quite similar to those of the Nb-Zr alloy, indicating that Nd had no effect on the conductivity and resistivity of Nb-Zr. Although Ce led to a decrease in the resistivity, the resistivity was rapidly improved via annealing.

Key Words **:** Nb-Zr Alloy, Electrical Resistivity, Thermal Diffusivity, Annealing Effects

1. Introduction

U-TRU-Zr metallic fuel is a candidate innovative fuel for the TRU burner [1, 2]. Americium (Am), one of the main targets of burning, will diffuse and form precipitates during operation. The matrix and thermal properties of metallic fuels will change, owing to neutron irradiation and annealing at high temperatures.

Thermal properties of this metallic fuel have been extensively studied, as simulations of the fuel temperature distribution require the precise thermal conductivity[2]. Post-irradiation examinations of various metallic fuel types, such as U-Zr or U-Pu-Zr alloys, have revealed that components of the fuel (especially Minor Actinides (MA) and Rare Earth (RE) elements) diffuse, thereby resulting in redistribution of the fuel matrix [3, 4].

Kim et al. have revealed the mechanism of this phenomenon[5]. The property changes caused by redistribution should be considered for precise performance simulation, but studies considering these changes are lacking.

Redistribution was mainly caused by neutron irradiation and chemical interaction between different elements. In metallic fuel, the main components, U and Zr, form a single phase at high temperatures (>700 °C), indicating that the van der Waals attraction between different elements is rather small. However, owing to a small attraction, sub-components of Am and RE will separate from U and Zr, and subsequently form an intermediate phase with plutonium, some other actinides, or another RE from fission products. Prior to loading U and Zr into a fast reactor, a U-TRU-Zr alloy forms a relatively homogeneous fuel matrix since the possible production procedure leads to quenching of the alloy [6]. The components of the metallic fuel will then diffuse slowly during the reactor operation.

Hence, chemical interactions play a key role in redistribution. In this study, Nb and RE (Ce and Nd)

* Advanced Interdisciplinary Science and Technology, Graduate School of Engineering
** Research Institute of Nuclear Engineering

were chosen as surrogates of U and Am, owing to the similarity between U/Zr and Am/Zr interactions. The chemical interaction and thermal effect were investigated by annealing each specimen as a simulation of reactor operation.

2. Surrogate material

As in the case of the U-Zr system, a body - centered - cubic (BCC) mixture phase forms in Nb-Zr binary systems heated at high temperatures. Metallic fuel production can be performed by quenching and loading the fuel into a fast reactor. Although the U-Zr system undergoes many phase transitions, the mixture phase should be present in the U-Zr metallic fuel prior to loading.

3. Experiment

Nb-22.2Zr alloys (same atomic ratio as the U-10Zr alloy) were prepared (by means of arc melting or quenching) with 5 wt.% addition of Ce or Nd.

Two samples with the same composition were produced from each Ce- and Nd-added alloy. Each sample was polished with SiC paper into a disc ($\emptyset$ = 10 mm, h $\leq$ 3 mm) for measurements of the thermal diffusivity, electrical resistivity, and composition. After the first measurement of these properties, the discs were annealed at 400 °C for 36, 120, and 240 h and the measurements of thermal diffusivity and electrical resistivity were then repeated.

The thermal diffusivity was measured via the laser flash method and was calculated as follows:

$$\alpha = 0.1388 * \frac{d^2}{t_{1/2}} \quad (1)$$

Where, α is the thermal diffusivity, d is the thickness of each specimen, and $t_{1/2}$ is the time corresponding to half of the maximum temperature. The thermal diffusivity under vacuum conditions at 300, 400, and 500 °C was evaluated via laser flash measurements, which lasted for nearly 4 h, i.e., for relatively shorter than the annealing time. Black bodies were obtained by spraying each specimen with graphite [7, 8].

A four-terminal method was used to assess the extremely low electrical resistivity of the alloy. The measured electric potential difference was converted into electrical resistivity and conductivity as follows:

$$\rho = F_0 \times F_1 \times F_2 \times \frac{V}{I} = 2\pi S * \frac{t/s}{2\ln\left\{\frac{\sinh(t/S)}{\sinh(t/2S)}\right\}} * \left[1 + \frac{1}{\ln 2} * \ln\left\{\frac{(d/s)^2+3}{(d/s)^2-3}\right\}\right] * \frac{V}{I} \quad (2)$$

$$\sigma = \frac{1}{\rho} \quad (3)$$

Where, σ is the electrical conductivity, ρ is the electrical resistivity, S is the distance (0.26 cm) between terminals corresponding to the measured potential difference, t and d are the thickness and diameter of the sample, respectively, V is the potential difference, and I is the current (0.3 A) [9]. The potential difference was measured at both surfaces of each disc. The electrometer and current were corrected before starting the measurement of each disc.

4. Results

4.1 Thermal Diffusivity

Figs. 1 to 3 show the thermal diffusivity of Nb-22.2Zr+RE (5 wt.% of Ce or Nd) for each disc at 300, 400, and 500 °C. Uncertainties of 5% were employed. At 300 °C, similar diffusivities were obtained for all specimens, except for the relatively high diffusivity of the Ce-added Nb-Zr alloy. The diffusivity of another Ce-added specimen was almost the same as that of the RE-free and Nd-added alloys and the diffusivity of Ce was lower than that of the Nb-Zr alloy. These results indicated that the high diffusivity of the Ce-added alloys lies within the measurement uncertainty. At 400 °C, consistent diffusivity was obtained for all the discs, but the results at 500 °C indicate an effect of RE addition, as

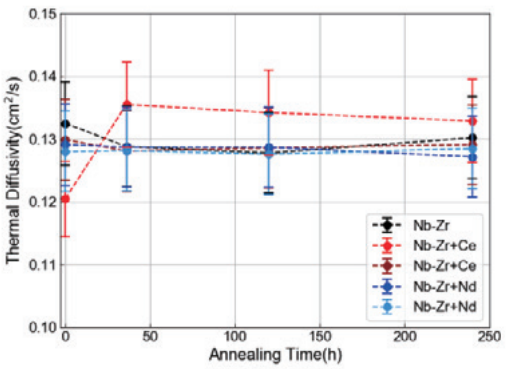

Fig. 1 Dependence of the thermal diffusivity at 300 ˚C on the annealing time. Error bar corresponds to ±5%

evidenced by the relatively large discrepancy obtained. However, the diffusivity of each sample varied inconsistently with the annealing time, i.e., the diffusivity measurement revealed no dependence of diffusivity on annealing time and RE addition.

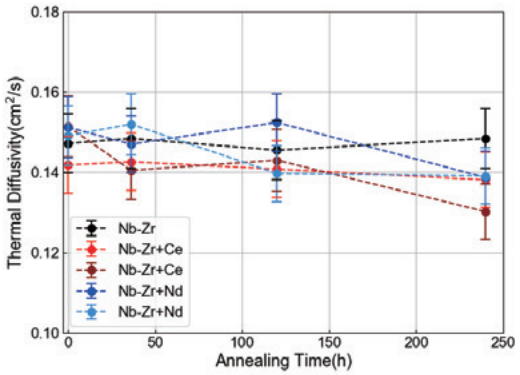

Fig.2 Dependence of the thermal diffusivity at 400 ˚C on the annealing time. Error bar corresponds to ±5% of the value

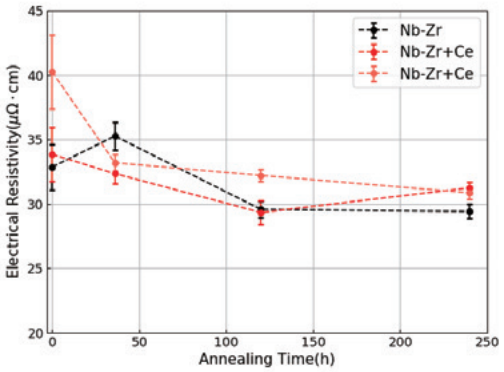

Fig.3 Dependence of the thermal diffusivity at 500 ˚C on the annealing time. Error bar corresponds to ±5% of the value.

4.2 Electrical Resistivity

Figs. 4 to 6 show the dependence of the electrical resistivity and conductivity at room temperature on the annealing time of each sample. The corresponding uncertainties were associated with the measurement points of each disc and contact situation. The resistivity of the RE-free and Nd-added alloys exhibited almost the same dependence on the annealing time, but the resistivity of the Ce-added alloy exhibited a different dependence. In one case, the conductivity was relatively lower than that of the RE-free alloy and was rapidly improved after 36 h of annealing. However, in the other case, the conductivity of the sample in the quenched

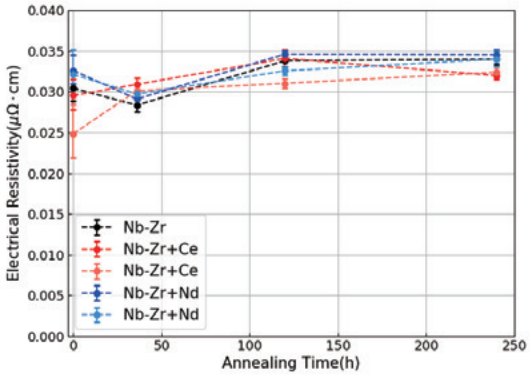

Fig.4 Dependence of the electrical resistivity on the annealing time of the Ce-added alloys. The error bars indicate the population variation statistically estimated from the measured value

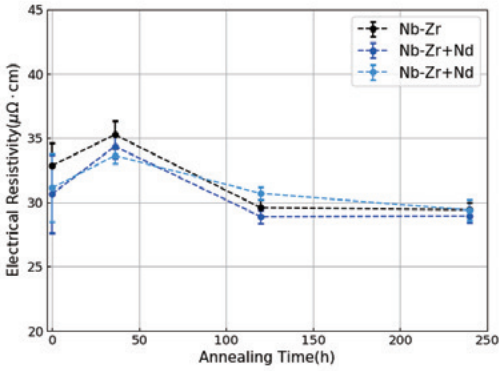

Fig.5 Dependence of the electrical resistivity on the annealing time of the Nd-added alloys. The error bars indicate the population variation statistically estimated from the measured value

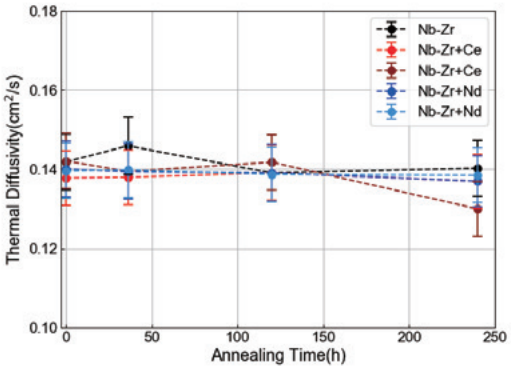

Fig.6 Dependence of the electrical resistivity on the annealing time of the Nb-Zr+RE alloys. The error bars indicate the population variation statistically estimated from the measured value

condition was almost the same as that of the other specimens.

4.3 Compositional Chages

Fig. 7 shows the content map obtained from SEM-EDS analyses of the Nb-Zr+Ce alloy (uncertainties were estimated from the measurement points and the SEM-EDS system). This map revealed a heterogeneous distribution of Ce (ranging from 1.5 wt.% to 4 wt.%) through the surface, indicating quite low solubility of Ce in the Nb-Zr alloy. Fig. 8 shows the compositional changes in each RE at the surface of each disc. As shown in the figure, the Ce content of the Ce-added alloys changed only slightly, whereas the Nd content of the Nb-Zr+Nd alloy increased significantly (from 2.5 wt.% to 4.2 wt.%). The difference between Ce addition and Nd addition may have resulted from the solubility difference of these metals. Massalski reported that, at 2640 K, the maximum solubility of Ce in Nb is 2.0 wt.%, whereas the solubility of Nd remains unknown [10]. However, similar trends observed for the RE solubility in other d-transition metals indicate that the maximum Nd solubility in Nb would be <1.5 wt.% at high temperatures. Mattern reported solubility values of ~12 wt.% at 1000 K and 7.7 wt.% at 1700 K for Ce and Nd, respectively, in solid Zr [10, 11]. From those published data and our SEM-EDS analyses, Ce and Nd solubility in Nb-Zr alloy was estimated as 2 wt.% to 3 wt.% and $\leq$2 wt.%, respectively. This suggested that, for RE amounts exceeding the solubility limit, the Nb-Zr alloy was unstable and excess RE diffused toward the grain boundary, thereby leading to equilibrium of the alloy.

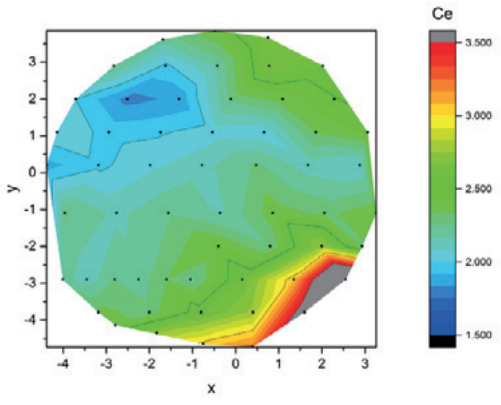

Fig.7 Ce content map of the disc surface

5. Discussions

The electrical conductivity and compositional changes exhibited strong dependences on the annealing time, whereas the thermal diffusivity exhibited no dependence.

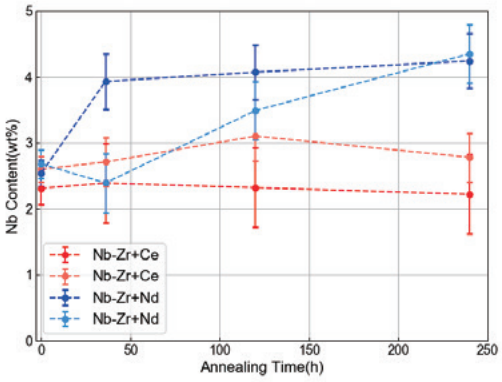

Fig.8 Dependence of RE on the annealing time at the surface. Error bar includes uncertainties associated with SEM-EDS and different areas of the sample.

The decrease in the electrical conductivity may have resulted from: (1) the shape of the sample, (2) the precipitation of oxide products, and (3) an increase in the amount of electron scattering induced by RE precipitation. The specimens were prepared via arc melting, where each specimen was polished from a button into a disc shape and, thus, different disc shapes were obtained. However, a correction was performed in order to obtain a finite disc shape of the specimens, based on the measured size. The conductivity varied with the shape of the samples. Furthermore, oxide products could be precipitated from RE, owing to the high reactivity of these elements. To verify this hypothesis, one of the Ce-added alloys was re-measured after polishing one side of the specimen with #2000 SiC paper. The re-measurement results were almost identical to the previous set of results. Therefore, the decrease in conductivity was attributed to an increase in the amount of electron scattering induced by RE precipitation (see point (3) from above).

We tried to determine the correlation between the compositional change and the electrical conductivity. Nb has the highest thermal conductivity of the elements considered in this experiment and, hence, we assumed that the Nb content at the surface is correlated with the conductivity. However, the results obtained for the compositional changes at the surface revealed that Nb is more distributed on the Ce-added alloy than on the Nd-added alloy. In addition, the maximum Nb concentration was realized after 120 h of annealing, although the electrical conductivity remained unchanged from the quenched state. This indicated that the Nb at the

surface had no correlation with the electrical conductivity. Similarly, the concentrations of Zr and RE were uncorrelated with the conductivity. That is, the Zr concentration differed significantly among the specimens, but the conductivity of the Nd-added alloy improved only modestly, whereas the Ce concentration changed only slightly, but the conductivity improved rapidly and significantly. We also considered the solubility difference. As previously mentioned in section 3.3., compared with Ce, Nd would have a relatively lower solubility in Nb and, hence, the main Nb-Zr phase contained a low amount of Nd.

6. Conclusion

The effect of annealing on the thermal diffusivity and electrical conductivity was determined for a Nb-Zr alloy with RE addition as a surrogate metallic fuel. The diffusivity of each RE-added specimen decreased at 500 °C. However, at 400 °C, similar diffusivity values were obtained, regardless of RE addition or annealing time.

The electrical conductivity of the quenched Ce-added alloy decreased at room temperature, but improved rapidly after a short annealing. However, as in the case of the RE-free Nb-Zr alloy, annealing-induced changes in the conductivities of the Nd-added alloys fell within the uncertainty limits.

For each disc, the dependence of the compositional changes on the annealing time was investigated via SEM-EDS. Compositional changes of Nd were detected, although the changes of Ce fell within the uncertainty limit. The difference between the behaviors of the Ce- and Nd-added alloys may have resulted from the difference between the solubility of these elements in the Nb-Zr alloy.

7. Acknowledgement

This research was conducted within the nuclear system research and development program under the auspices of the Ministry of Education, Culture, Sports, Science and Technology (MEXT) in Japan during fiscal years 2014 to 2017. The project title was “Innovative metallic fuel design and development of the production technology for TRU burning”.

References

[1] K. Arie, Y. Tsubota, T. Oomori *et al.*, in *Proceedings of GLOBAL*. (2015).

[2] T. Nishi, K. Nakajima, M. Takano *et al.*, "Thermal conductivity of U-20 wt.%Pu-2 wt.%Am-10 wt.%Zr alloy". *Journal of Nuclear Materials* **464** (2015). 270-274,10.1016/j.jnucmat.2015.04.043.

[3] M. K. Meyer, S. L. Hayes, W. J. Carmack *et al.*, "The EBR-II X501 minor actinide burning experiment". *Journal of Nuclear Materials* **392** (2009). 176-183,10.1016/j.jnucmat.2009.03.041.

[4] C. Sari, C. T. Walker, M. Kurata *et al.*, "Interaction of U-Pu-Zr alloys containing minor actinides and rare earth with stainless steel". *Journal of Nuclear Materials* **208** (1994) 201-210.

[5] Y. S. Kim, S. L. Hayes, G. L. Hofman *et al.*, "Modeling of constituent redistribution in U-Pu-Zr metallic fuel". *Journal of Nuclear Materials* **359** (2006) 17-28,10.1016/j.jnucmat.2006.07.013.

[6] T. Ogata, "Metal Fuel" in "Comprehensive Nuclear Materials", chap. 3. 01, Elsevier (2012).

[7] W. J. Parker, R. J. Jenkins, C. P. Butler *et al.*, "Flash Method of Determining Thermal Diffusivity, Heat Capacity, and Thermal Conductivity". *Journal of Applied Physics* **32** (1961). 1679-1684,10.1063/1.1728417.

[8] L. Vozár, W. Hohenauer, "Uncertainty of Thermal Diffusivity Measurements Using the Laser Flash Method". *International Journal of Thermophysics* **26** (2005) 1899-1915,10.1007/s10765-005-8604-5.

[9] S. Yilmaz, "The geometric resistivity correction factor for several geometrical samples". - *Journal of Semiconductors* **36** (2015) 082001, 10.1088/1674-4926/36/8/082001.

[10] N. Mattern, Y. Yokoyama, A. Mizuno *et al.*, "Experimental and thermodynamic assessment of the Ce-Zr system". *Calphad-Computer Coupling of Phase Diagrams and Thermochemistry* **46** (2014) 213-219,10.1016/j.calphad.2014.05.002.

[11] N. Mattern, Y. Yokoyama, A. Mizuno *et al.*, "Experimental and thermodynamic assessment of the Nd-Zr system". *Calphad-Computer Coupling of Phase Diagrams and Thermochemistry* **46** (2014) 103-107,10.1016/j.calphad.2014.02.008.